

The comparison of alternative spacetimes using the spherical accretion around the black hole

Orhan Donmez

*College of Engineering and Technology, American University of the Middle East,
Egaila 54200, Kuwait.*

orhan.donmez@aum.edu.kw

Received (Day Month Year)

Revised (Day Month Year)

In the region where the gravitational field is strong, we have examined the influence of different gravities on the accretion disk formed due to spherical accretion. To achieve this, we obtain numerical solutions of the GRH equations, utilizing Schwarzschild, Kerr, Einstein-Gauss-Bonnet, and Hartle-Thorne spacetime metrics. We investigate the impact of the rotation parameter of a black hole (a/M), the EGB coupling constant (α), and the quadrupole moment of the rotating black hole (q) on the accretion disk formed in a strong field. The formation of the disk for the slowly and rapidly rotating black hole models is separately examined, and comparisons are made. Our numerical simulations reveal that, under the specific conditions, the solution derived from Hartle-Thorne gravity converges towards solutions obtained from Kerr and other gravitational models. In the context of the slowly rotating black hole with $a/M = 0.28$, we observe a favorable agreement between the Hartle-Thorne result and the Kerr result within the range of $0 < q < 0.5$. Conversely, in the scenario of the rapidly rotating black hole, a more pronounced alignment with the value of $q = 1$ is evident within the range of $0.5 < q < 1$. Nevertheless, for $q > 1$, it becomes apparent that the Hartle-Thorne solution diverges from solutions provided by all gravitational models. Our motivation here is to utilize the Hartle-Thorne spacetime metric for the first time in the numerical solutions of the GRH equations for the black holes, compare the results with those obtained using other gravities, and identify under which conditions the Hartle-Thorne solution is compatible with known black hole spacetime metric solutions. This may allow us to provide an alternative perspective in explaining observed X -ray data.

Keywords: numerical relativity; rotating black hole; Hartle-Thorne gravity; gravitational collapse; EGB gravity.

PACS Nos.: include PACS Nos.

1. Introduction

The observation and analysis of X -ray emissions are crucial steps in explaining astrophysical systems and their behaviors. For instance, uncovering the physical characteristics of known and observed compact objects in the universe, understanding the interactions with accretion disks around them, and finding the physical properties of jets formed as a result of the interaction between the compact object and the disk are significant strides in unraveling the mysteries of the universe. Thus,

known X -ray binaries and active galactic nuclei (AGN) can be fully understood.¹⁻⁴

Understanding the accretion disk around compact objects plays a crucial role in unraveling the mysteries of the universe. The accretion disk serves as a laboratory environment for astrophysical systems, contributing to the explanation of many events occurring in the universe.^{5,6} Through this disk, it is possible to comprehend various phenomena, from the formation of celestial objects to understanding the behavior of matter in environments where strong gravitational forces are present.^{7,8} In the accretion disk around black holes, matter interacting with the black hole converts a certain amount of substance into energy, leading to emission. These emissions are observable, and spectral analyses of these radiations can reveal the characteristics of the compact object at the center.⁹

After the gravitational collapse, stable black holes can form, and around these holes, they can create accretion disks.¹⁰ Black holes at the center are characterized by their mass and angular momentum. The mathematical definition of this black hole was provided by Kerr by solving Einstein's equations.^{11,12} Later, Gauss-Bonnet gravity was defined as another solution to Einstein's equations.^{13,16,17} In this gravity, the mass of the central black hole is determined based on its angular momentum and the Gauss-Bonnet coupling constant. Using both gravities, it has been observed that a stable disk is formed around the newly created black hole as a result of spherical accretion.^{14,15} In this article, in addition to the spacetime matrices mentioned above, we will examine the behavior of an accretion disk around a slowly rotating compact object, using the Hartle-Thorne spacetime, which is believed to behave like Kerr and EGB gravities¹⁸. We will also compare the results of these three gravities.

The Hartle-Thorne metric is a solution to Einstein's equations and describes the spacetime around a slowly rotating compact object. This spacetime matrix defines both the object itself and the surrounding curvature. Using this spacetime matrix, astrophysical events related to the rotation of compact objects can be characterized.^{18,19} Thus, the structure of accretion disks formed around slowly rotating but deformed black holes can be revealed. The Hartle-Thorne spacetime varies based on the object's mass, angular, and quadrupole moments. These parameters characterize different astrophysical systems.²⁰⁻²² When characterized using the quadrupole moment expression, the Hartle-Thorne metric transforms into the Kerr metric.

The Hartle-Thorne metric is widely used in the literature to describe the structure of slowly rotating neutron stars and the phenomena occurring around them. Ref. 22 has worked on determining the equations of state compatible with the observed frequency pairs from the source 4U 1636-53 using the Hartle-Thorne geometry. In doing this, the Resonant Switch model developed for these twin frequency states has been utilized. Thus, based on the compatibility of the Hartle-Thorne metric and the equations of state, the mass, rotation parameters, and quadrupole parameter describing the neutron star and its surrounding geometry for the source 4U 1636-53 have been determined. The conversion of the Hartle-Thorne metric into

the Kerr metric is also crucial for understanding the phenomena surrounding rotating black holes. This transformation is applicable in modeling accretion disks around black holes and in comprehending their diverse behaviors. The dynamic structure of the shock cone formed by Bondi-Hoyle-Lyttleton accretion around the Hartle-Thorne black hole has also been revealed in cases with both slowly and rapidly rotating black holes. Then, the quasi-Periodic-Oscillations trapped within this shock cone were extracted. According to the results obtained in Ref. 23, the Hartle-Thorne black hole has the potential to explain the QPOs observed from some sources. Therefore, in addition to known gravitational theories, it can be used to explain physical phenomena and QPO oscillations observed in binary black hole systems.

The application of the Hartle-Thorne metric to systems with a rotating central black hole may be crucial in explaining certain physical events.²⁴ Alternatively, in some systems where we assume a central black hole, it may reveal the presence of slowly rotating stars at the center. Addressing these questions is an important area of research. For this purpose, predictions made through numerical calculations are significant alongside theoretical models. It has been observed that the results obtained from numerical models for the $a/M = 0.5$ value of the neutron star are consistent with the Hartle-Thorne metric.²⁴ This underscores the importance of understanding the disk structures around black holes and comparing them with results obtained from Kerr and EGB black holes.

In this study, we aim to model accretion disks evolving around Schwarzschild, Kerr, EGB, and Hartle-Thorne black holes, generated as a consequence of spherical accretion. In this novel approach, we aim to simulate the accretion disk encircling rotating black holes by employing the Hartle-Thorne spacetime metric. By doing so, we anticipate uncovering distinct gravitational effects on the disk around black holes through the application of the Hartle-Thorne metric, which was initially designed for slowly rotating neutron stars. This undertaking has the potential to yield fresh perspectives and a more profound comprehension of the astrophysical phenomena unfolding near rotating black holes, thereby enhancing our understanding of general relativity in highly gravitational settings. Our investigation takes into account physical variables such as mass accretion rates, variations in disk density, the radial velocity of the infalling matter, and other physical properties of the disk, considering both slow and fast-rotating black holes. Subsequently, we will compare the results of Schwarzschild, Kerr, and EGB black holes with each other, as well as compare the results obtained from the Hartle-Thorne solution with those obtained from these models. Lastly, through a comparison of numerical results with analytical solutions, we seek to elucidate certain astrophysical phenomena. To achieve this, we numerically model the GRH equations using four different spacetime matrices.

After providing matrices that define Hartle-Thorne, Kerr, and EGB black holes and the curvature of spacetime around them in Chapter 2, we briefly defined the General Relativistic hydrodynamic equations on the equatorial plane. In Chapter 3, we described the physical characteristics of matter sent from the outer bound-

ary of the computational domain toward the black hole, forming a global accretion disk around the black hole. Additionally, in this chapter, we defined the outflow boundary condition that allows matter reaching the inner boundary to fall into the black hole. Furthermore, in this chapter, we demonstrated how the horizon of the black hole changes depending on the rotation parameter a/M and the quadrupole moment q in the case of Hartle–Thorne gravity. In Chapter 4, we extensively discussed the numerical results of the accretion disk formed around slowly and rapidly rotating black holes in different gravity scenarios. In the same chapter, we compared Hartle–Thorne gravity with Kerr gravity, discussing at which value of q in Hartle–Thorne approaches to the Kerr gravity. Finally, in Chapter 5, we summarize the obtained numerical results and compare with the literature.

Throughout the entire paper, unless explicitly stated otherwise, the convention of using geometrized units where c and G are set to 1 is adhered to. All the parameters used in this article are dimensionless. They all vary proportionally with the mass of the central black hole. Therefore, the results obtained here can be applied to stellar or massive black holes. Only by using the mass of the black hole at the center of the applied system, a conversion is made from geometrized units to the SI unit system. Subsequently, the numerical results obtained can be compared with observational outcomes.

2. Equations

2.1. Hartle-Thorne Spacetime Metric

The Hartle-Thorne spacetime represents a solution to Einstein’s field equations in vacuum, providing a description of the curved spacetime surrounding a rotating black hole. This metric accurately accounts for the mass quadrupole moment ($q = Q/M^3$) to first order and the angular momentum ($a = J/M^2$) to second order where M is the mass of the black hole. The spacetime metric pertains to a slowly rotating black hole with nearly spherical characteristics. Utilizing this metric in General Relativity and Hydrodynamics equations offers a valuable avenue to investigate the behavior of matter and understand the accretion mechanisms occurring in the strong gravitational region near the event horizon of the rotating black hole.²³

The line element of the Hartle-Thorne spacetime reads^{18, 23, 25}

$$ds^2 = - \left(1 - \frac{2M}{r}\right) \left(1 + 2f_1 P_2(\text{Cos}\theta) + 2 \left(1 - \frac{2M}{r}\right)^{-1} \frac{J^2}{r^4} (2\text{Cos}^2\theta - 1)\right) dt^2 \\ + \left(1 - \frac{2M}{r}\right)^{-1} \left(1 - 2f_2 P_2(\text{Cos}\theta) - 2 \left(1 - \frac{2M}{r}\right)^{-1} \frac{J^2}{r^4}\right) dr^2(1) \\ - \frac{4J}{r} \text{Sin}^2\theta dt d\phi + r^2 [1 - 2f_3 P_2(\text{Cos}\theta)] d\theta^2 r^2 [1 - 2f_3 P_2(\text{Cos}\theta)] \text{Sin}^2\theta d\phi^2,$$

where $P_2(\text{Cos}\theta) = \frac{1}{2} (3\text{Cos}^2\theta - 1)$, $f_1 = \frac{J^2}{Mr^3} \left(1 + \frac{M}{r}\right) + \frac{5}{8} \frac{qM^3 - J^2/M}{M^3} Q_2^2 \left(\frac{r}{M} - 1\right)$,

The comparison of alternative spacetimes using the spherical accretion around the black hole 5

$f_2 = f_1 - \frac{6J^2}{r^4}$, $f_3 = f_1 + \frac{J^2}{r^4} + \frac{5}{4} \frac{qM^3 - J^2/M}{M^2(r^2 - 2Mr)^{1/2}} Q_2^1 \left(\frac{r}{M} - 1 \right)$. $P_2(\text{Cos}\theta)$ is the second Legendre polynomial of the first kind. Q_2^1 and Q_2^2 are the associated Legendre Polynomials of the second kind which are $Q_2^1 = (x^2 - 1)^{1/2} \left(\frac{3x}{2} \ln \frac{x+1}{x-1} - \frac{3x^2-2}{x^2-1} \right)$ and $Q_2^2 = (x^2 - 1) \left(\frac{3}{2} \ln \frac{x+1}{x-1} - \frac{3x^3-5x^2}{x^2-1} \right)$ as a function of x which is $x = \frac{r}{M} - 1$.

In order to solve the GRH equations using the spacetime matrix, we need to define the lapse function and shift vectors in the Hartle-Thorne coordinates. The relation between 4-metric g_{ab} , 3-metric γ_{ij} , lapse function and shift vectors given as²⁶

$$\begin{pmatrix} g_{tt} & g_{ti} \\ g_{it} & \gamma_{ij} \end{pmatrix} = \begin{pmatrix} (\beta_k \beta^k - \alpha^2) & \beta_k \\ \beta_i & \gamma_{ij} \end{pmatrix}, \quad (2)$$

where $i, j, k = 1, 2$ and 3 . After doing straightforward calculation, the lapse function for Hartle-Thorne spacetime metric is

$$\alpha = \sqrt{\frac{4J^2}{r^4(1+f_3)} - \left(1 - f_1 - \frac{2J^2}{r^4 \left(1 - \frac{2M}{r} \right)} \right) \left(\frac{2M}{r} - 1 \right)}, \quad (3)$$

the components of the shift vectors are

$$\beta_r = 0, \quad \beta_\theta = 0, \quad \beta_\phi = -\frac{2J}{r} \quad (4)$$

As previously mentioned, the external Hartle-Thorne geometry can be described using three parameters, namely the black hole mass (M), the dimensionless angular momentum (a), and the dimensionless quadrupole moment (q).

2.2. Kerr and EGB Spacetime Matrices

One of the general objectives of this article is to compare the results obtained for the accretion disks modeled using the Hartle-Thorne geometry with the results previously found in the Kerr and Einstein-Gauss-Bonnet (EGB) gravity scenarios. Therefore, briefly, the spacetime matrices for Kerr and EGB gravities are provided below with supporting references. Utilizing various matrices in numerical computations further enables us to investigate the implications of alternative gravitational theories, as demonstrated in previous studies.^{15, 27-30}

The Kerr black hole exhibits an exceptionally potent gravitational force owing to its rotational parameter, simultaneously distorting the spacetime in its vicinity. Specifically, when investigating the characteristics of material within the inner disk region, the Kerr metric is the appropriate choice. The Kerr black hole's metric in Boyer-Lindquist coordinates is defined as follows:^{11, 12, 31}

6 *Orhan Donmez*

$$ds^2 = - \left(1 - \frac{2Mr}{\Sigma^2} \right) dt^2 - \frac{4Mra}{\Sigma^2} \sin^2 \theta dt d\phi + \frac{\Sigma^2}{\Delta_1} dr^2 + \Sigma^2 d\theta^2 + \frac{A}{\Sigma^2} \sin^2 \theta d\phi^2 \quad (5)$$

where $\Delta_1 = r^2 - 2Mr + a^2$, and $A = (r^2 + a^2)^2 - a^2 \Delta \sin^2 \theta$. In Boyer-Lindquist coordinates, the shift vector and lapse function of the Kerr metric are given by: Shift vector (β^i): $\beta^t = 0$, $\beta^r = 0$, and $\beta^\theta = \frac{-2Mar}{A}$. The lapse function is $\tilde{\alpha} = \sqrt{\frac{\Delta_1}{A}}$.

Einstein-Gauss-Bonnet (EGB) gravity is a distinct solution within the framework of Einstein's equations, offering an alternative gravitational theory. Unlike Kerr gravity, this alternative theory features the presence of an alpha (α) parameter. The influence of this parameter, particularly when investigated in proximity to black holes, can be harnessed to provide explanations for observed phenomena. The α parameter introduces higher curvature corrections, thereby providing a novel viewpoint on the behavior of black holes under extreme conditions and within higher-dimensional spacetime.³² EGB metric is^{13,29,33}

$$ds^2 = - \frac{\Delta_2 - a^2 \sin^2 \theta}{\Sigma} dt^2 + \frac{\Sigma}{\Delta_2} dr^2 - 2a \sin^2 \theta \left(1 - \frac{\Delta_2 - a^2 \sin^2 \theta}{\Sigma} \right) dt d\phi + \Sigma d\theta^2 + \sin^2 \theta \left[\Sigma + a^2 \sin^2 \theta \left(2 - \frac{\Delta_2 - a^2 \sin^2 \theta}{\Sigma} \right) \right] d\phi^2, \quad (6)$$

where $\Sigma = r^2 + a^2 \cos^2 \theta$, $\Delta_2 = r^2 + a^2 + \frac{r^4}{2\alpha} \left(1 - \sqrt{1 + \frac{8\alpha M}{r^3}} \right)$. In this context, a , α , and M correspond to the black hole's spin parameter, Gauss-Bonnet coupling constant, and its mass, respectively. The lapse function is $\tilde{\alpha} = \sqrt{\frac{a^2(1-f(r))^2}{r^2+a^2(2-f(r))} + f(r)}$ and the shift vectors are $\beta^i = \left(0, \frac{ar^2}{2\pi\alpha} \left(1 - \sqrt{1 + \frac{8\pi\alpha M}{r^3}} \right), 0 \right)$. The variable $f(r)$ is defined as $f(r) = 1 + \frac{r^2}{2\alpha} \left(1 - \sqrt{1 + \frac{8\alpha M}{r^3}} \right)$. The gamma matrix, denoted as $\gamma_{i,j}$ in the GRH equations, defines three-dimensional space and is derived from the metrics g_{ab} for both Kerr and EGB gravities. In this context, the Latin indices i and j vary from 1 to 3.

2.3. General Relativistic Hydrodynamic Equations

During gravitational collapse, a fluid, such as gas or dust, is drawn toward a massive object, such as a black hole, neutron star or massive star, by gravitational forces and accumulates around it. This phenomenon plays a crucial role in comprehending the interaction between matter and black hole, as well as other dense entities in the universe. The examination of the gravitational collapse of a perfect fluid in the vicinity of black holes, particularly the Kerr, Einstein-Gauss-Bonnet (EGB), and Hartle-Thorne black holes, involves solving General Relativistic Hydrodynamical (GRH) equations within a curved background. The perfect fluid stress-energy-momentum tensor is given as

The comparison of alternative spacetimes using the spherical accretion around the black hole 7

$$T^{ab} = \rho h u^a u^b + P g^{ab}, \quad (7)$$

g^{ab} , ρ , u^a , p , and h , are the three-metric of the curved spacetime the rest-mass density, the 4- velocity of the fluid, the fluid pressure, and the specific enthalpy, respectively. The indices a , b , and c range from 0 to 3.

In order to numerically solve the GRH equations, it is essential to represent them in a conserved form:³⁴

$$\frac{\partial U}{\partial t} + \frac{\partial F^r}{\partial r} + \frac{\partial F^\phi}{\partial \phi} = S. \quad (8)$$

The vectors U , F^r , F^ϕ , and S correspond to the conserved variables, fluxes along the r and ϕ directions, and sources, respectively. These conserved variables are defined in relation to the primitive variables, as illustrated below,

$$U = \begin{pmatrix} D \\ S_r \\ S_\phi \\ \tau \end{pmatrix} = \begin{pmatrix} \sqrt{\gamma} W \rho \\ \sqrt{\gamma} h \rho W^2 v_r \\ \sqrt{\gamma} h \rho W^2 v_\phi \\ \sqrt{\gamma} (h \rho W^2 - P - W \rho), \end{pmatrix} \quad (9)$$

where the term $h = 1 + \epsilon + P/\rho$ represents the enthalpy, the expression $W = (1 - \gamma_{a,b} v^i v^j)^{-1/2}$ denotes the Lorentz factor, $v^i = u^i/W + \beta^i$ represents the three-velocity of the fluid. ϵ represents the internal energy. The fluid pressure is calculated using the ideal gas equation of state. The three-metric $\gamma_{i,j}$ and its determinant γ are determined based on the four-metric of black hole. Latin indices i and j vary from 1 to 3. The flux and source terms can be computed for any metric using the following equations,

$$\vec{F}^i = \begin{pmatrix} \tilde{\alpha} \left(v^i - \frac{1}{\tilde{\alpha} \beta^i} \right) D \\ \tilde{\alpha} \left(\left(v^i - \frac{1}{\tilde{\alpha} \beta^i} \right) S_j + \sqrt{\gamma} P \delta_j^i \right) \\ \tilde{\alpha} \left(\left(v^i - \frac{1}{\tilde{\alpha} \beta^i} \right) \tau + \sqrt{\gamma} P v^i \right) \end{pmatrix} \quad (10)$$

and,

$$\vec{S} = \begin{pmatrix} 0 \\ \tilde{\alpha} \sqrt{\gamma} T^{ab} g_{bc} \Gamma_{aj}^c \\ \tilde{\alpha} \sqrt{\gamma} (T^{a0} \partial_a \tilde{\alpha} - \tilde{\alpha} T^{ab} \Gamma_{ab}^0) \end{pmatrix} \quad (11)$$

where Γ_{ab}^c is the Christoffel symbol.

<i>Model</i>	<i>type</i>	$\alpha(M^2)$	a/M	q
<i>SCH</i>	<i>Schwarzschild</i>	–	–	–
<i>K028</i>	<i>Kerr</i>	–	0.28	–
<i>K09</i>		–	0.9	–
<i>K028_EGB1</i>		0.68	0.28	–
<i>K028_EGB2</i>		–3.03	0.28	–
<i>K028_EGB3</i>	<i>Gauss – Bonnet</i>	–4.93	0.28	–
<i>K09_EGB1</i>		0.05	0.9	–
<i>K09_EGB2</i>		–3.61	0.9	–
<i>K028_HT1</i>		–	0.28	0
<i>K028_HT2</i>	<i>Hartle – Thorne</i>	–	0.28	1
<i>K028_HT3</i>		–	0.28	3
<i>K028_HT4</i>		–	0.28	5
<i>K09_HT1</i>		–	0.9	0
<i>K09_HT2</i>	<i>Hartle – Thorne</i>	–	0.9	1
<i>K09_HT3</i>		–	0.9	3
<i>K09_HT4</i>		–	0.9	6

3. Initial and Boundary Conditions

Here, using the Hartle-Thorne metric, we examine the disk of matter that spreads around the newly formed compact object due to gravitational collapse, revealing the structures of this disk. By comparing the obtained results with those from other gravity models such as Kerr and Gauss-Bonnet, we determine the effects of alternative gravity. To perform these comparisons, we numerically solve these metrics in the General Relativistic Hydrodynamic (GRH) equations.^{34–36} While solving these equations, we assume that matter behaves like an ideal gas and use $P = (\Gamma - 1)\rho\epsilon$ with $\Gamma = 4/3$.

Initially, we assume that the computational domain around the black hole is empty. Therefore, during the definition of this region, we consider it to have negligible density and pressure, and these values should be exceedingly small. While making these choices, density and pressure values are determined with the consideration that the speed of sound should be $C_\infty = 0.1$. The same selection is applied to the initial values used when matter is sent into the computational domain from outer boundary. For the formation of the disk around the black hole, gas from the outer boundary is injected with values $V^r = -0.01$, $V^\phi = 0$, and $\rho = 1$.¹⁴ Calculations are performed on the equatorial plane. Detailed descriptions of the initial models for Kerr, Gauss-Bonnet, and Hartle-Thorne black hole, can be found in Table 1.

The grid employs uniformly spaced zones in both the radial and angular directions, with 1024 zones in the radial direction and 256 zones in the angular direction. The inner boundary of the computational domain is situated at $r_{min} = 3.7M$, while the outer boundary extends to $r_{max} = 100M$ along the radial axis. Angular boundaries are defined as $\phi_{min} = 0$ and $\phi_{max} = 2\pi$. In this article, we investigate the behavior of matter falling towards a black hole through accretion in order to reveal the effects of different gravities on the region near the black hole horizon. Therefore, it is necessary for the inner boundary of the computational domain to be as close to the black hole horizon as possible. However, the location of the horizon of EGB black holes varies entirely depending on the α parameter. For instance, when $\alpha = 0.6$, the horizon is around $r = 1M$, whereas when $\alpha = -4.93$, the horizon is

at $r = 3.5M$. Consequently, to ensure a fair comparison, the inner radius of the computational domain is set to $r = 3.7M$ in each model.

The code is executed until the time ($t_{max} = 30000M$), which significantly surpasses the time ($\sim 5000M$) required for the model to reach a steady state. It has been ascertained that crucial aspects of the numerical solutions, such as instabilities, the presence of quasi-periodic oscillations (QPOs), the location of shocks, and the behavior of accretion rates, remain largely unaffected by variations in grid resolution.^{15, 28, 29, 33}

The accurate definition of boundaries in numerical modeling prevents unwanted oscillations. Thus, the characteristics of oscillations arising from black hole-disk interactions can be revealed. Otherwise, unwanted residues from the boundary can create both non-physical situations and lead to the crash of the code.¹⁴ Here, to model the proposed disk, we aim for matter near the inner boundary, close to the black hole, to fall towards the black hole. This is because once matter crosses the last stable orbit, it is impossible for it to escape from the black hole. Therefore, an outflow boundary condition is applied here. On the other hand, according to the proposed model, it is assumed that the supernovae remnants continuously fall towards the black hole. As a result, matter is injected at the outer boundary of the disk, which is far from the black hole.

In Fig.1, the variation of the radius of the compact object defined by the Hartle-Thorne gravity is shown according to q and a/M . The left part of the figure illustrates the change in radius with respect to q in different a/M conditions. Each thick black vertical line represents the change in radius for a different a/M . Here, it is clearly seen that as q increases, the radius increases. However, the growth of a/M , as in the Kerr spacetime matrix, has reduced the radius. This confirms that the Hartle-Thorne metric behaves similarly to Kerr.¹⁸ On the other hand, the right part of the figure shows how the radius changes with a/M . Each point corresponding to the thick lines in the vertical direction, where a/M is constant, corresponds to different q . This indicates that increasing q increases the radius. Again, it is clearly seen here that increasing a/M reduces the radius. Finally, it has been observed that the value of a/M corresponding to each q is not between 0 and 1. In other words, there is a certain range of physically defined a/M for each q . The reverse is also true. However, it has been observed that as q increases, the number of possible values for a/M increases. In other words, to be able to choose a/M anywhere between 0 and 1, q must be sufficiently large.

4. The Numerical Simulation of the Spherical Accretion

The accretion disks are important mechanisms to describe the physical characteristics of the black hole at the center. Understanding the properties of the electromagnetic emissions emitted by the disks is necessary to comprehend the characteristics of black holes. For decades, scientists have been working to understand the enigmatic creatures of the universe and black holes by using theoretical, numerical, and

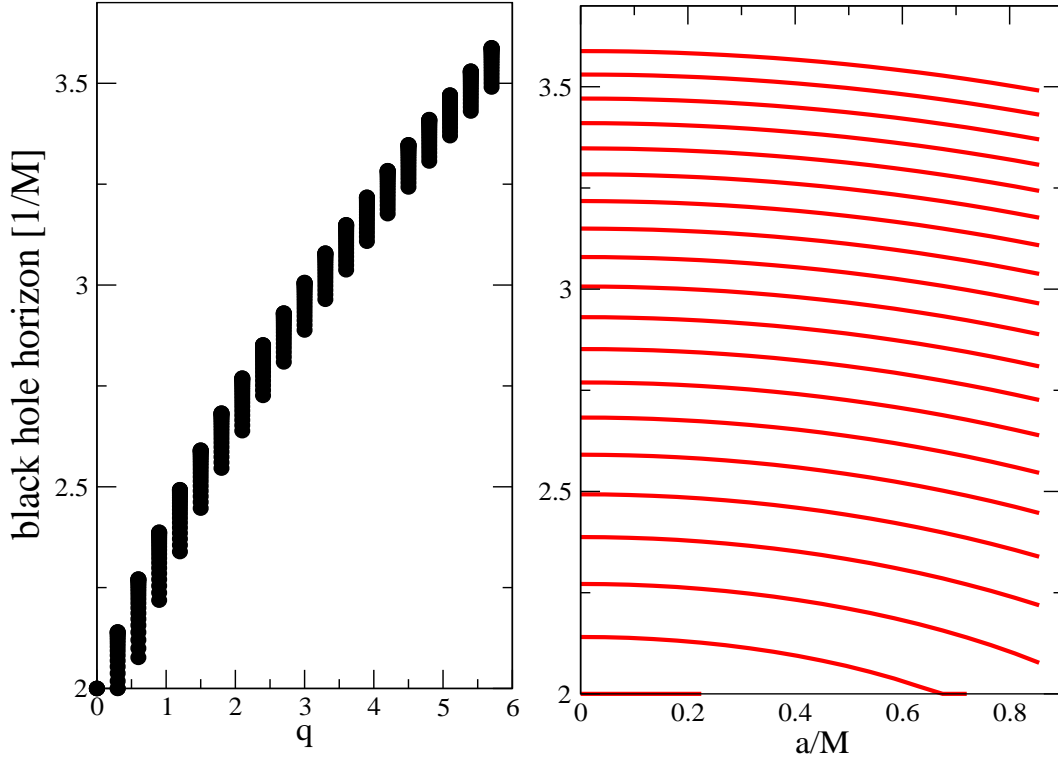


Fig. 1. The change in the black hole's horizon depending on the black hole's spin (a/M) and quadrupole parameter (q). The left panel shows the change in the black hole's horizon for each a/M as a function of q while the right one illustrates the change in the horizon for each q as a function of a/M .

observational methods. Important observations have been attempted to understand the physical characteristics of the black holes at the centers of the Milky Way and *M87* galaxies, especially through significant observations made by the Event Horizon Telescope (EHT) in recent years.^{37,38} Particularly, observations indicate that the geometry around black holes has certain limitations.⁵ In this context, numerical and theoretical studies are crucial to contribute to observational results. Many studies have been conducted, especially in revealing the characteristics of accretion disks around Schwarzschild and Kerr black holes, both theoretically and numerically.^{5, 6, 39, 40}

In recent years, with the definition of 4D EGB gravity,²⁷ theoretical^{41–48} and numerical studies^{28,29} the dynamic structures of accretion disks around the *EGB* black holes and the resulting *QPO* oscillations continue. Additionally, adapting Hartle-Thorne gravity, which is an important gravity in describing the behavior of

matter around neutron stars, to black holes and conducting theoretical^{18,19,24} and numerical studies in this direction can provide a different approach to explaining disk characteristics and observational data. In this context, the theoretical investigation of the structure of the disk around an Hartle-Thorne black hole has begun, and the support of this by numerical relativity would be a significant advancement in the field. This is because Hartle-Thorne gravity is an important theory in explaining slowly rotating deformed objects in regions where the gravity is very strong.^{18,19} Thus, by examining the three crucial parameters characterizing a black hole—mass, angular momentum, and quadrupole moment in the context of Hartle-Thorne gravity, certain astrophysical system characteristics can be revealed.^{20,21}

Comparing Hartle-Thorne gravity with Kerr and EGB ones, it has some advantages, especially in terms of its flexibility.¹⁸ In the absence of angular momentum, it characterizes a naked singularity. If there are angular momentum and a quadrupole moment, it behaves like the Kerr metric. For these reasons and other things mentioned above, the Hartle-Thorne metric applied to the black holes in recent years. Modeling the disk around black holes with Hartle-Thorne Horndeski gravity could open a different perspective in explaining observational data. By numerically solving the GRH equations using this Hartle-Thorne metric, we reveal how the parameters of an accretion disk behave in different gravities in the following sections.

4.1. Slowly Rotating Black Hole: $a/M=0.28$

The rest-mass density resulting from spherical accretion can be used to explain many physical events occurring due to the interaction of the black hole with its accretion disk. In other words, information about the mass density can be derived to understand the physical characteristics and types of electromagnetic radiation observed by detectors resulting from this interaction. The rest-mass density is also related to the mass accretion rate of the spherical accretion around the black hole. The density obtained as matter falls towards the black hole provides information about the amount of matter falling into the black hole. Thus, an estimate can be made about the mass increase rates of the black holes. For these reasons, numerically calculated rest-mass density using different gravities provides us with information about the spacetime curvature around the black hole. This is why, in Fig.2, we showed how the mass density of the disk around the slowly rotating black holes changes radially and axially using the different gravities.

The left part of Fig.2 shows how the density changes in the azimuthal direction at $r = 4M$ for the slowly rotating black hole model with $a/M = 0.28$. As expected, since the disk is obtained through global accretion, the density remains constant. However, the density exhibits different behaviors for different gravities and the parameters associated with those gravities, as anticipated. This, as mentioned above, contributes to the variations observed in the data and the change in the mass of the central black hole. In the right panel of Fig.2, the variation of the disk's density with respect to r is shown for different gravities and parameters. As expected, due

to the strong gravitational field, the density of the disk has exponentially increased as it approaches the black hole horizon.

In the Fig.2, the variation in mass resulting from the use of Kerr, Schwarzschild, and other gravities is provided. Since the black hole is the slowly rotating, the results for Kerr and Schwarzschild are close to each other. EGB gravity exhibits different behavior for extreme positive and negative values of α , corresponding to this rotation parameter. When $\alpha = 0.68$, the mass density is greater than Kerr, and for negative values of α , it is smaller than Kerr. Interestingly, at $\alpha = -4.93$, it is observed that the density is slightly larger than Kerr again in the strong gravitational region (very close to the horizon). This is related to the intensive chaos occurred during the black hole-matter interaction and it was also mentioned in our previous calculations.^{15, 29, 49} However, as seen in the right panel of Fig.2, it has been observed that as we move away from the black hole's horizon, this value is still smaller than Kerr.

On the other hand, the behavior of the disk's density in Hartle-Thorne gravity is compared to Kerr gravity. As seen in the Fig.2, at $q = 0$, the maximum density of the disk is greater than the Kerr case, but at $q = 1$, this density is smaller than Kerr. It is clearly seen that as the q value increases, the density becomes smaller compared to Kerr, indicating a departure from the Kerr value. In conclusion, as understood from this graph, in Hartle-Thorne gravity, it can be said that it approaches Kerr for the range of $0 < q < 1$. More specifically, it can be inferred that it is compatible with Kerr when the q is slightly less than 0.5.

To observe how much different gravities deviate from Kerr, or in other words, the deviation ratios from Kerr, we normalized the results obtained from all models with Kerr. This situation is presented in Fig.3. As seen here, in the $q = 0$ case, the rest-mass density has produced a solution closer to Kerr, while this deviation is more significant in the $q = 1$ case. As mentioned above, for a value of q in the range $0 < q < 0.5$, we can say that the Hartle-Thorne solution transforms to Kerr. Again, as seen in Fig.3, interestingly, for large negative α values in EGB gravity, it exhibits similar behavior to Hartle-Thorne with larger q . However, while the deviation of EGB gravity results occurs around Kerr, for large values of q , the results gradually move away from the Kerr solution.

The mass accretion rate is directly related to the matter density around a black hole. A higher mass accretion implies that the disk is hotter, leading to the production of high-energy radiation. On the other hand, a higher mass accretion means more matter falling into the black hole, resulting in a decrease in the rest-mass density of the disk. Mass accretion, and consequently the rest-mass density, is associated with the luminosity of the disk. Therefore, changes in the mass accretion rate in different gravitational scenarios lead to variations in the observed data. These variations are depicted in the left part of Fig.4. In Hartle-Thorne gravity, as the q value increases (for example, $q = 5$), and in EGB gravity, for large negative values of α (for example, $\alpha = -3.03$ and -4.93), the mass accretion rate significantly deviates from other models. However, models other than these exhibit similar mass

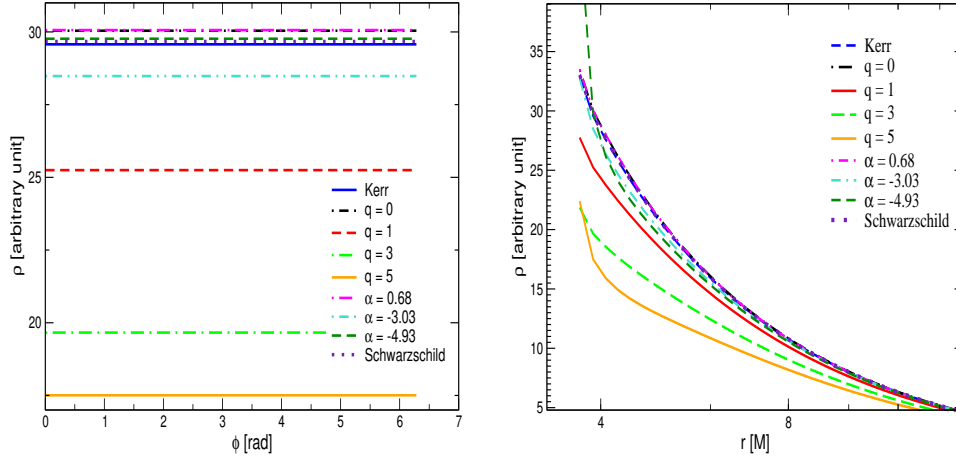


Fig. 2. In the case of a black hole with a spin parameter of $a/M = 0.28$, the variation of density with respect to position at $t = 30000M$. On the left graph, the density variation with respect to ϕ for the accretion disk is shown, while on the right, it is illustrated how this density changes with r . In both cases, the density variation is compared for different gravities and their respective parameters.

accretion rates, meaning they can produce similar luminosity.

The graph on the right side of Fig.4 illustrates the radial velocity of matter falling towards the black hole as a function of r . This allows the estimation of the conversion rate from gravitational potential energy, created by the black hole on the matter, to kinetic energy. Additionally, the radial velocity shows that in the region where the gravitational force is high, i.e., in the region where the potential well created by spacetime is deepest, the flow velocity of matter decreases. Again, it is observed that the Hartle-Thorne result for $0 < q < 0.5$ might be consistent with Kerr solution.

4.2. Rapidly Spinning Black Hole: $a/M=0.9$

Although Hartle-Thorne gravity describes the spacetime around a slowly rotating deformed compact object, comparing the results obtained from Hartle-Thorne gravity for cases with high rotation parameters to other gravitational theories and Kerr may help us better understand not only slowly rotating black hole systems but also provide an opportunity to compare different gravitational theories in such scenarios. The numerical modeling of accretion disk around the black hole in Hartle-Thorne gravity may be utilized to explain certain astrophysical phenomena in the case of a rapidly rotating black hole. Considering both the rapid rotation and deformation of the black hole can be crucial in understanding such scenarios. In this situation,

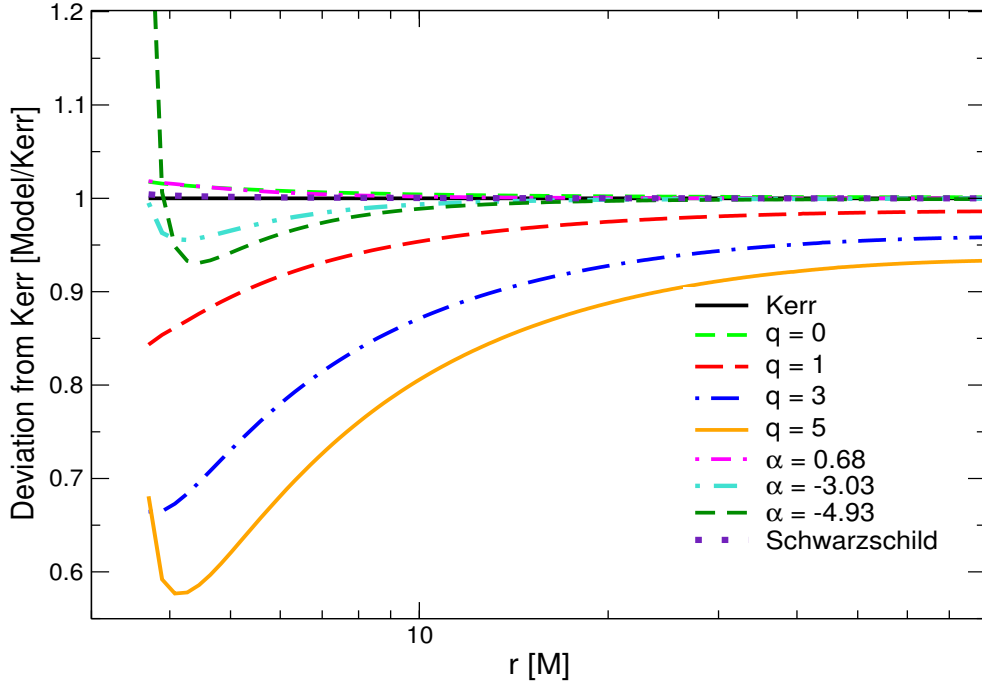


Fig. 3. The same as Fig.2, but this time comparing the radial disk density for each gravity after normalization with Kerr solution. In the presence of different gravities, the radial variation of the density of the accretion disk formed through spherical accretion around a black hole is compared with the disk density around a Kerr black hole.

unraveling the behavior of globally accreting matter can contribute significantly to the literature. On the other hand, the primary goal of Hartle-Thorne gravity, which is actually to examine the behavior of matter around a deformed compact object rather than the rotation parameter, can also be explored in the context of the impact of the rotation parameter. Therefore, in this section, the accretion disk around a rapidly rotating Hartle-Thorne black hole is modeled, and the results are compared with different gravitational models in the presence of the rapid rotation parameter.

We compared different gravities with the Kerr model for the rapidly rotating black hole scenario with $a/M = 0.9$, drawing the rest-mass density in both the azimuthal and radial directions. The left part of Fig.5 illustrates the change in density with respect to ϕ . Again, as expected, the disk density remains constant along the ϕ at $r = 4M$. However, it is evident that the rest-mass density takes different values around the Kerr model for different gravities and their associated parameters. The significant variation in the rest-mass density clearly indicates that

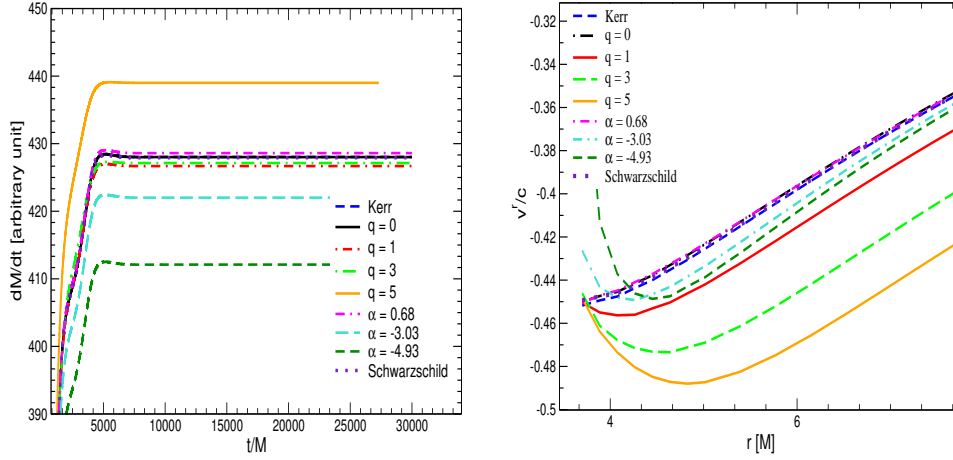


Fig. 4. The same as Fig.2, but the variation of the mass accretion rate of the disk formed around a slowly rotating black hole and the radial variation of the infalling matter’s radial velocity towards the black hole are provided.

different gravities, and consequently the black holes, introduce differences in the dynamical structure of the accretion disk, leading to potential oscillations, radiation, and variations in luminosity.

As seen in Fig.5, within the rapidly rotating black hole model, the Hartle-Thorne solution exhibits variation around the Kerr solution for the range of $0 < q < 1$ for the quadrupole moment parameter. Upon closer examination, it is observed that the disk’s rest-mass density approaches the Kerr solution as q approaches 1. Therefore, it is anticipated that when the quadrupole moment parameter is close to 1, the numerical solution obtained from the Hartle-Thorne gravity would be closer to the Kerr solution. However, for $q = 0$ and $q > 1$, the solutions obtained from Hartle-Thorne gravity models deviate from the Kerr solution. Simultaneously, when comparing the results obtained from Hartle-Thorne gravity with Schwarzschild, EGB, and Kerr, it can be stated that the disk density at $r = 4M$ takes similar values. The deviation occurs only in the cases of $q = 0$ and $q > 1$.

For the rapidly rotating black hole model, the deviation ratio from the Kerr black hole is presented in Fig.6. As observed, the minimum deviation from the Kerr solution for our models is noted at $q = 1$, in line with the previously mentioned observation that the quadrupole moment parameter in the range of $0.5 < q < 1$ produces a solution similar to Kerr. However, for $q = 0$ and $q > 1$, the solutions significantly diverge from Kerr solution.

On the other hand, in EGB gravity, the $\alpha = 0.05$ provides a solution almost similar to Schwarzschild. Generally, EGB gravity exhibits behavior similar to Kerr

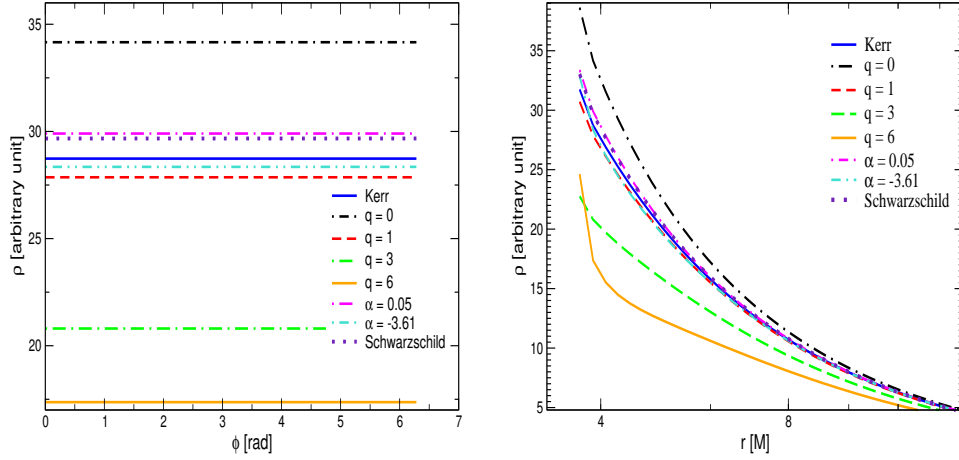


Fig. 5. The same as Fig.2 but it is for a spin parameter of $a/M = 0.9$.

for possible positive²⁹ values of α and $\alpha > -4$, as seen in the slow rotating black hole model. Conversely, for extremely negative values of α , as observed in this comparison, the deviation from Kerr is substantial. Additionally, in this comparison, it is evident that EGB gravity with large negative α values shows similar behavior to Hartle-Thorne with large q , especially in the region near the black hole's horizon. However, the deviation ratios from Kerr differ significantly between these two gravities for bigger q . This similar behavior in both gravities can be utilized to explain emissions occurring in strong gravitational fields and their physical mechanisms.

Falling matter's radial velocity towards a black hole provides crucial information about the structure of the accretion disk and the behavior of matter. The transformation of the disk's angular momentum or the emission of generated energy can be deduced from it. Details about the amount of matter residing on the disk, the ratio of matter falling toward the black hole, and whether the disk is hot or cold can be inferred. Therefore, knowing the radial velocity is important when comparing different gravities. This way, based on the characteristics of observed data, the effects of gravity can be revealed, or the presence of a particular gravity can be identified. In Fig.7, the variation of radial velocity with respect to r for different gravities is shown according to the parameters used in the models. For Hartle-Thorne gravity, again, the best fit with Kerr is observed from the results obtained for the $q = 1$ model. As previously mentioned, other q values deviate significantly from Kerr results, as clearly depicted in the figure. Our comparisons and results from the previous paragraph are evident in this figure. Particularly for $q > 1$ and large negative values of α , it is observed that the matter slows down as it approaches the black hole.

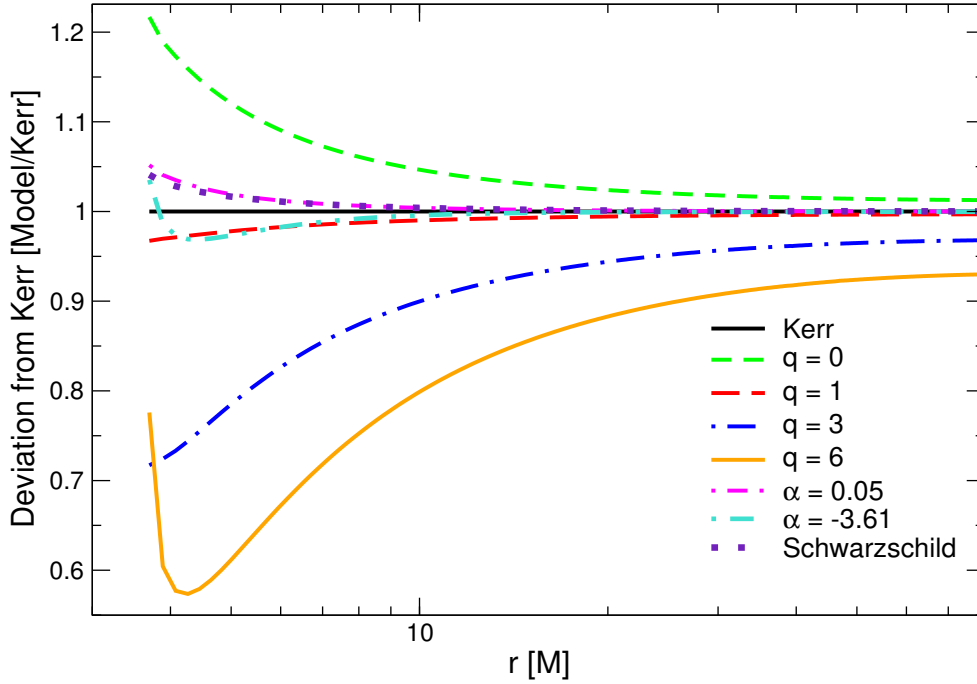


Fig. 6. The same as Fig.3 but it is for a spin parameter of $a/M = 0.9$.

4.3. Comparison of Slowly and Rapidly Spinning Black Holes in The Hartle-Thorne gravity

The Hartle-Thorne metric is a solution to the Einstein field equations for compact objects and typically describes the spacetime around a slowly rotating Kerr black hole. It is a gravity solution obtained by expanding the metric that defines the space for a fully rotating black hole, taking into account higher-order terms in a series. It is generally applied in cases where the angular momentum of the black hole is small.

In this study, to demonstrate that the Hartle-Thorne metric can be used even in cases of high rotation parameters of a black hole, a stable disk formed around the black hole is modeled. In Fig.8, the radial variation of the disk's density, dependent on the quadrupole moment q , is shown for a black hole model with a rotation parameter of $a/M = 0.9$ using the Hartle-Thorne metric and compared with the Kerr black hole solution. As seen in Fig.8, for a slowly rotating black hole with $a/M = 0.28$, the $q = 0$ provides a result close to the Kerr solution, while other q values deviate from the Kerr solution. On the other hand, for $a/M = 0.9$, the

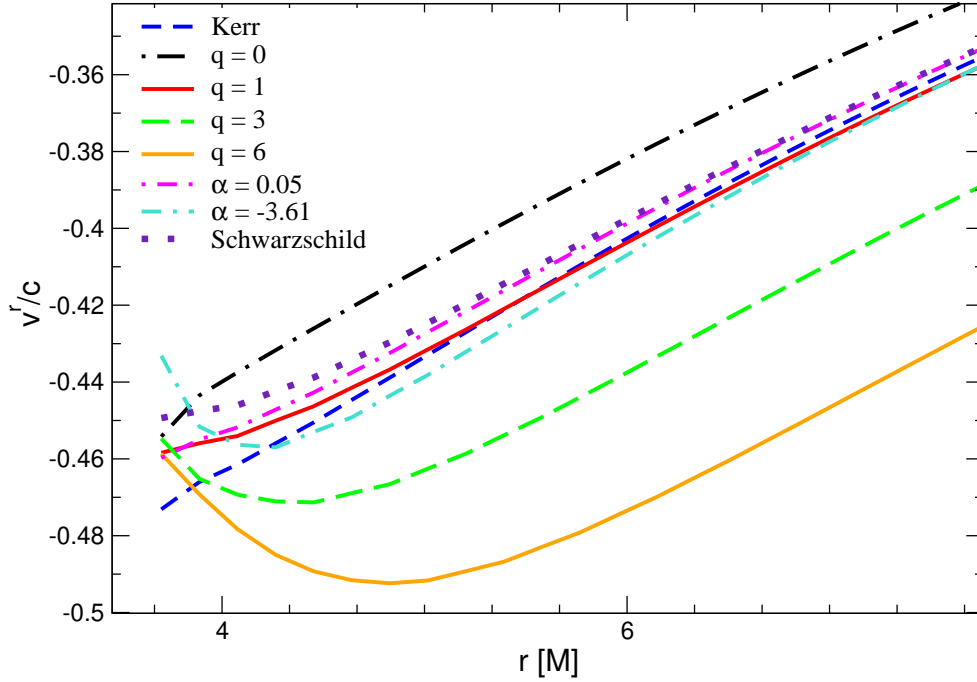


Fig. 7. The same as Fig.4 only for the radial velocity of the matter falling toward the black hole but it is for a spin parameter of $a/M = 0.9$.

solution obtained from Hartle-Thorne gravity at $q = 1$ is closer to the Kerr solution. However, for q values other than 1, the deviation is significant and increases as the value of q increases.

According to these initial results, the Hartle-Thorne metric can be used for the rapidly rotating black holes, but q should be different for a given specific a/M . If the result obtained from the Hartle-Thorne gravity is desired to transform into the Kerr solution, q should increase as a/M increases. On the other hand, the results obtained from Hartle-Thorne gravity produce different results from Kerr for different values of a/M and q . For q values other than $q = q_{Kerr}$, which are compatible with Kerr for Hartle-Thorne gravity, either the density of the disk is greater or less than Kerr. In the case of $q < q_{Kerr}$, the rest-density of the disk around the black hole increases, while in the case of $q > q_{Kerr}$, this density decreases. This can alter the physical characteristics of radiation in a regions with a strong gravitational field.

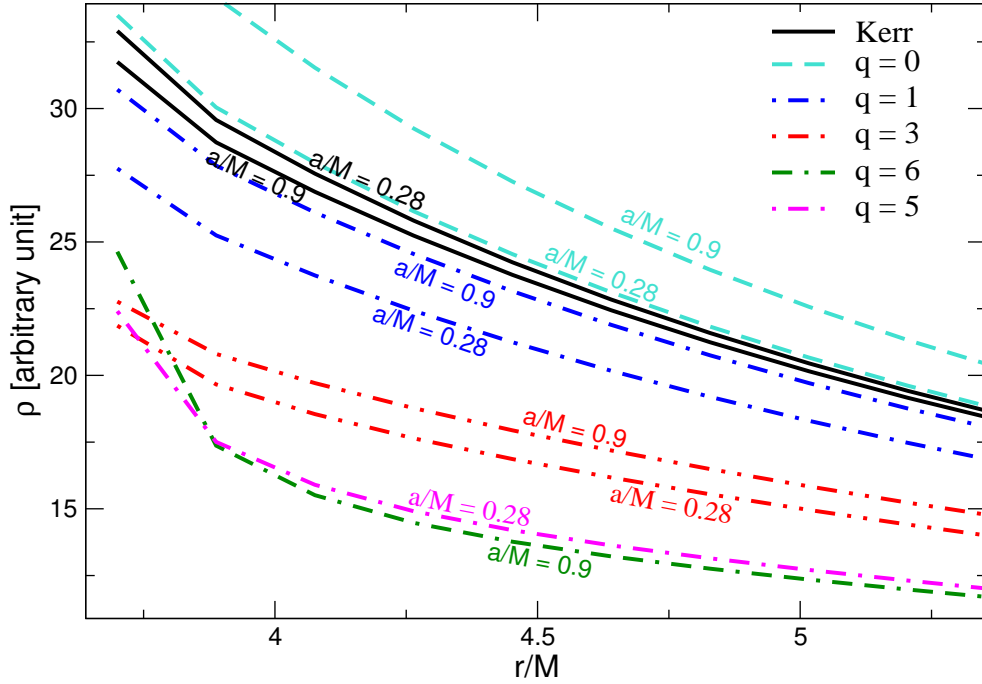


Fig. 8. Accretion disk density variation with respect to r for different a/M and q values in Kerr and Hartle-Thorne gravities. The agreement and differences between the results obtained using the Kerr spacetime and the calculated density of the disk for different q values have been highlighted. It is observed that the density of the disk undergoes significant changes with different values of q .

5. Discussion and Conclusion

In this study, we modeled the accretion disk around the black holes formed through the spherical accretion by numerically solving the GRH equations using Schwarzschild, Kerr, EGB, and Hartle-Thorne gravities. Our modeling is conducted in $2D$ on the equatorial plane. When determining the model types, we consider possible different values of parameters defining these gravities for both slowly rotating and rapidly rotating black holes. Thus, we systematically conduct a study by considering the impact of α in EGB gravity and the quadrupole moment in Hartle-Thorne gravity, along with the rotation parameter of the black hole, on the formation and dynamic structure of the disk in different gravities.

To unveil the dynamic structure of the disk, we calculate the angular and radial variations in disk density, the mass accretion rate of matter falling toward the black hole, and the radial velocity of matter as it falls toward the black hole through spacetime. By doing so, we reveal the dynamic structure of the disk and

the behavior of matter around the black hole that could shed light on observational data. Simultaneously, we compared the outcomes of the disk's behavior in different gravities by normalizing them with Kerr.

According to the results from our numerical modeling, it has been observed that different parameters defining gravity, namely α and q , play an effective role in the formation of the disk around a slowly rotating black hole with $a/M = 0.28$. The results obtained from Hartle-Thorne are found to be consistent with Kerr for the range $0 < q < 1$. Moreover, it is anticipated that the Hartle-Thorne solution could align with Kerr when the value of q is around 0.5 or closer to $q = 0$. On the other hand, for $q \geq 1$, it is noticed that the results deviate from those obtained from Kerr. As q increases, this deviation is observed to grow. In fact, when $q = 5$, it is determined that the radial velocity of the disk decreases near the black hole horizon. In other words, as q increases, there seems to be a significant change in the behavior of the parameters responsible for the formation of the disk. Furthermore, a comparison is made between EGB gravity and Kerr for the case $a/M = 0.28$. Although the results in this gravity do not deviate from Kerr as much as in the case of Hartle-Thorne, it is observed that near the black hole horizon, the change in density at a large negative α value is similar to the behavior of the large q value in Hartle-Thorne.

The Hartle-Thorne gravity is generally formulated to describe the spacetime around slowly rotating black holes. However, in this study, we have extended our analysis by comparing the results obtained from Hartle-Thorne for a rapidly rotating black hole (specifically, $a/M = 0.9$) with Kerr and EGB gravities. This comparison is motivated by the belief that it may provide insights into certain astrophysical phenomena that remain unexplained in black hole observations. The numerical simulations reveal that the disk's behavior around rapidly rotating black holes yields a solution that is closest to Kerr when $q = 1$ in Hartle-Thorne gravity. In essence, this suggests compatibility between Kerr and Hartle-Thorne solutions for values of q slightly less than 1. Conversely, for both $q = 0$ and $q > 1$, it becomes evident that Hartle-Thorne deviates from the Kerr solution. Analogous to the scenario of a slowly rotating black hole model, in Hartle-Thorne gravity with $q = 6$ and EGB gravity with $\alpha = -3.61$, despite both gravities exhibiting similar behavior near the black hole's horizon, the EGB solution aligns much more closely with the Kerr solution.

In conclusion, the results obtained in this study and the comparison of the Hartle-Thorne solution with various gravities, particularly for slow and rapidly rotating black hole models, can be further expanded to encompass wider ranges of q . This extension would facilitate the identification of the specific values of q at which the Hartle-Thorne solution undergoes a transformation into the Kerr solution. A more detailed application of Hartle-Thorne gravity to black hole models could significantly contribute to elucidating certain astrophysical systems characterized by unclear physical mechanisms.^{20,21}

Acknowledgments

All simulations were performed using the Phoenix High Performance Computing facility at the American University of the Middle East (AUM), Kuwait.

Data availability

The data used in the article are entirely composed of data obtained by running our own program, which solves the General Relativistic Hydrodynamics Equations, on a High-Performance Computer. Each model has generated about 4GB of data. Since the total number of models is 19 given in Table 1, this means a total of 36GB of data. Data can be sent to the requested people through private communication.

References

1. Max Camenzind. Book review: Compact Stellar X-Ray Sources / Cambridge University Press, 16 + 690 pp., ISBN 0-521-82659-4 (2006). *Sterne und Weltraum*, 45(10):89–90, October 2006.
2. T. M. Tauris and E. P. J. Van Den Heuvel. Formation and evolution of compact stellar X-ray sources. In *Compact Stellar X-ray Sources*, page 623. 2010.
3. Hagai Netzer. Revisiting the Unified Model of Active Galactic Nuclei. *ARAA*, 53:365–408, August 2015.
4. Françoise Combes. In *Active Galactic Nuclei*, 2514-3433. IOP Publishing, 2021.
5. Marek A. Abramowicz and P. Chris Fragile. Foundations of Black Hole Accretion Disk Theory. *Living Reviews in Relativity*, 16(1):1, January 2013.
6. Matias Montesinos. Review: Accretion Disk Theory. *arXiv e-prints*, page arXiv:1203.6851, March 2012.
7. D.N.C. Lin and J.C.B. Papaloizou. Theory of accretion disks ii: Application to observed systems. *Annual Review of Astronomy and Astrophysics*, 34(1):703–747, 1996.
8. Hajime Inoue. X-ray observations of accretion disks. *PASJ*, 74(1):R1–R44, February 2022.
9. G. J. M. Luna, K. Mukai, J. L. Sokoloski, A. B. Lucy, G. Cusumano, A. Segreto, M. Jaque Arancibia, N. E. Nuñez, R. E. Puebla, T. Nelson, and F. Walter. X-ray, UV, and optical observations of the accretion disk and boundary layer in the symbiotic star RT Crucis. *AAP*, 616:A53, August 2018.
10. Suresh C. Jaryal and Ayan Chatterjee. Spherical Gravitational Collapse in 4D Einstein- Gauss- Bonnet theory. *arXiv e-prints*, page arXiv:2204.13358, April 2022.
11. Charles W. Misner, Kip S. Thorne, and John Archibald Wheeler. *Gravitation*. 1973.
12. Bernard Schutz. *A First Course in General Relativity*. 2009.
13. Dražen Glavan and Chunshan Lin. Einstein-Gauss-Bonnet Gravity in Four-Dimensional Spacetime. *PRL*, 124(8):081301, February 2020.
14. Orhan Donmez. The gravitational collapse of the dust toward the newly formed rotating black holes in Kerr and 4-D Einstein-Gauss-Bonnet Gravities. *arXiv e-prints*, page arXiv:2307.11725, July 2023.
15. Orhan Donmez. Perturbing the Stable Accretion Disk in Kerr and 4-D Einstein-Gauss-Bonnet Gravities:Comprehensive Analysis of Instabilities and Dynamics. *arXiv e-prints*, page arXiv:2310.13847, October 2023.
16. Abdelghani Errehymy, S. K. Maurya, G. Mustafa, Sudan Hansraj, H. I. Alrebdy, and

22 *Orhan Donmez*

- Abdel-Haleem Abdel-Aty, Black Hole Solutions with Dark Matter Halos in the Four-Dimensional Einstein-Gauss-Bonnet Gravity *Fortsch. Phys.*, 71(10-11), 2300052 2023.
17. S. K. Maurya, Abdelghani Errehymy, Ksh. Newton Singh, Nuha Al-Harbi, Kottakaran Sooppy Nisar, Abdel-Haleem Abdel-Aty, Minimally deformed anisotropic stars in dark matter halos under EGB-action *European Physical Journal C*, 83(10), 968, 2023.
 18. Yergali Kurmanov, Marco Muccino, Kuantay Boshkayev, Talgar Konysbayev, Orlando Luongo, Hernando Quevedo, and Ainur Urazalina. Accretion disk in the Hartle-Thorne spacetime. *arXiv e-prints*, page arXiv:2306.15050, June 2023.
 19. Kyriakos Destounis and Kostas D. Kokkotas. Slowly-rotating compact objects: the nonintegrability of Hartle-Thorne particle geodesics. *General Relativity and Gravitation*, 55(11):123, November 2023.
 20. N. Andersson and G. L. Comer. Slowly rotating general relativistic superfluid neutron stars. *Classical and Quantum Gravity*, 18(6):969–1002, March 2001.
 21. Nikolaos Stergioulas. Rotating Stars in Relativity. *Living Reviews in Relativity*, 6(1):3, June 2003.
 22. Stuchlík, Z. and Urbanec, M. and Kotrlovà, A. and Török, G. and Goluchová, K. Equations of State in the Hartle-Thorne Model of Neutron Stars Selecting Acceptable Variants of the Resonant Switch Model of Twin HF QPOs in the Atoll Source 4U 1636-53. *acta*, 65(2):169-195, June 2015.
 23. Donmez, Orhan and Dogan, Fatih The Shock Cone Instabilities and Quasi-Periodic Oscillations around the Hartle–Thorne Black Hole. *Universe*, 10(4):152, March 2024.
 24. Gabriela Urbancová, Martin Urbanec, Gabriel Török, Zdeněk Stuchlík, Martin Blaschke, and John C. Miller. Epicyclic Oscillations in the Hartle-Thorne External Geometry. *APJ*, 877(2):66, June 2019.
 25. H. T. Cromartie, E. Fonseca, S. M. Ransom, P. B. Demorest, Z. Arzoumanian, H. Blumer, P. R. Brook, M. E. DeCesar, T. Dolch, J. A. Ellis, R. D. Ferdman, E. C. Ferrara, N. Garver-Daniels, P. A. Gentile, M. L. Jones, M. T. Lam, D. R. Lorimer, R. S. Lynch, M. A. McLaughlin, C. Ng, D. J. Nice, T. T. Pennucci, R. Spiewak, I. H. Stairs, K. Stovall, J. K. Swiggum, and W. W. Zhu. Relativistic Shapiro delay measurements of an extremely massive millisecond pulsar. *Nature Astronomy*, 4:72–76, January 2020.
 26. C. W. Misner, K. S. Thorne, and J. A. Wheeler. *Gravitation. Volume I* 1977.
 27. Sushant G. Ghosh and Rahul Kumar. Generating black holes in 4D Einstein-Gauss-Bonnet gravity. *Classical and Quantum Gravity*, 37(24):245008, December 2020.
 28. Donmez, Orhan. Bondi-hoyle accretion around the non-rotating black hole in 4d einstein-gauss-bonnet gravity - bondi-hoyle around egb black hole. *Eur. Phys. J. C*, 81(2):113, 2021.
 29. O. Donmez. Dynamical evolution of the shock cone around 4D Einstein-Gauss Bonnet rotating black hole. *Physics Letters B*, 827:136997, April 2022.
 30. Donmez, Orhan. Bondi-Hoyle-Lyttleton Accretion around the Rotating Hairy Horn-deski Black Hole. *arXiv:2402.16707*, 2024.
 31. O. Dönmez, O. Zanotti, and L. Rezzolla. On the development of quasi-periodic oscillations in Bondi-Hoyle accretion flows. *MNRAS*, 412(3):1659–1668, April 2011.
 32. Pedro G. S. Fernandes, Pedro Carrilho, Timothy Clifton, and David J. Mulryne. The 4D Einstein-Gauss-Bonnet theory of gravity: a review. *Classical and Quantum Gravity*, 39(6):063001, March 2022.
 33. Orhan Donmez, Fatih Dogan, and Tuba Sahin. Study of Asymptotic Velocity in the Bondi–Hoyle Accretion Flows in the Domain of Kerr and 4-D Einstein–Gauss–Bonnet Gravities. *Universe*, 8(9):458, September 2022.

34. Orhan Dönmez. Code Development of Three-Dimensional General Relativistic Hydrodynamics with AMR (Adaptive-Mesh Refinement) and Results from Special and General Relativistic Hydrodynamics. *APSS*, 293(3):323–354, September 2004.
35. O. Dönmez. Relativistic simulation of flip-flop instabilities of Bondi-Hoyle accretion and quasi-periodic oscillations. *MNRAS*, 426(2):1533–1545, October 2012.
36. Orhan Donmez. Solution of the 1D Special Relativistic Hydrodynamics(SRH) Equations Using Different Numerical Method and Results from Different Test Problems. *AM&C*, 181(1):256–270, September 2006.
37. Event Horizon Telescope Collaboration et.al. First M87 Event Horizon Telescope Results. I. The Shadow of the Supermassive Black Hole. *APJL*, 875(1):L1, April 2019.
38. Event Horizon Telescope Collaboration et.al. First M87 Event Horizon Telescope Results. II. Array and Instrumentation. *APJL*, 875(1):L2, April 2019.
39. Sandip K. Chakrabarti, K. Acharyya, and D. Molteni. Quasi-Periodic Oscillations in Numerical Simulation of Accretion Flows Around Black Holes. *arXiv e-prints*, pages astro-ph/0211516, November 2002.
40. Fahrettin Koyuncu and Orhan Dönmez. Numerical simulation of the disk dynamics around the black hole: Bondi-Hoyle accretion. *Modern Physics Letters A*, 29(21):1450115, June 2014.
41. Jia-Xi Feng, Bao-Min Gu, and Fu-Wen Shu. Theoretical and observational constraints on regularized 4D Einstein-Gauss-Bonnet gravity. *arXiv e-prints*, page arXiv:2006.16751, June 2020.
42. Yu-Peng Zhang, Shao-Wen Wei, and Yu-Xiao Liu. Spinning Test Particle in Four-Dimensional Einstein-Gauss-Bonnet Black Holes. *Universe*, 6(8):103, July 2020.
43. Shafqat Ul Islam, Rahul Kumar, and Sushant G. Ghosh. Gravitational lensing by black holes in the 4d einstein-gauss-bonnet gravity. *Journal of Cosmology and Astroparticle Physics*, 2020(09):030–030, sep 2020.
44. Rahul Kumar and Sushant G. Ghosh. Rotating black holes in 4D Einstein-Gauss-Bonnet gravity and its shadow. *JCAP*, 2020(7):053, July 2020.
45. Sushant G. Ghosh, Arun Kumar, and Dharm Veer Singh. Anti-de Sitter Hayward black holes in Einstein-Gauss-Bonnet gravity. *Physics of the Dark Universe*, 30:100660, December 2020.
46. Shao-Wen Wei and Yu-Xiao Liu. Testing the nature of Gauss-Bonnet gravity by four-dimensional rotating black hole shadow. *arXiv e-prints*, page arXiv:2003.07769, March 2020.
47. Mohaddese Heydari-Fard, Malihe Heydari-Fard, and Hamid Reza Sepangi. Thin accretion disks around rotating black holes in 4D Einstein-Gauss-Bonnet gravity. *European Physical Journal C*, 81(5):473, May 2021.
48. Mohaddese Heydari-Fard and Hamid Reza Sepangi. Thin accretion disk signatures of scalarized black holes in Einstein-scalar-Gauss-Bonnet gravity. *Physics Letters B*, 816:136276, May 2021.
49. Orhan Donmez. Proposing a Physical Mechanism to Explain Various Observed Sources of QPOs by Simulating the Dynamics of Accretion Disks around the Black Holes. *arXiv e-prints*, page arXiv:2311.08388, November 2023.

